The use of alcohols to quench the reaction is not recommended because they do not dissolve sodium hyponitrite and may cause the latter to coat any unreacted pieces of sodium present in the mixture. A related literature preparation with pyridine[43] gave an impure, pyrophoric product. Two other procedures[44,45] for making sodium hyponitrite have succeeded in our laboratory but have not been used on a routine basis.

Laser Photolysis. All laser photolysis experiments were carried out under oxygen-free conditions. The samples (typically 1 mL) were excited with the pulses from a Molectron UV-24 nitrogen laser. Our system has been fully interfaced with a PDP11/03L computer which controls the experiments, gathers the data, and provides suitable processing, storage, and hardcopy facilities. Further details have been published elsewhere.[20]

Acknowledgment. Thanks are due to Mr. S. E. Sugamori for his technical assitance. One of us (G.D.M.) thanks the National Research Council of Canada for the support as a guest worker.

Registry No. *t*-BuON=NOBu-*t*, 14976-54-6; $Ph(CH_3)CHON{=}NOCH(CH_3)Ph$, 82522-46-1; $(CH_3)_2CHON{=}NOCH(CH_3)_2$, 82522-47-2; *c*-$C_6H_{11}ON{=}NO$-*c*-$C_6H_{11}$, 82522-48-3; $PhCH_2ON{=}NOCH_2Ph$, 19657-56-8; $PhCH_2CH_2ON{=}NOCH_2CH_2Ph$, 82522-49-4; *t*-BuO·, 3141-58-0; *c*-$C_6H_{11}O$·, 3384-35-8; $PhCH_2O$·, 26397-37-5; $PhCH_2CH_2O$·, 40355-55-3; *p*-methoxyacetophenone, 100-06-1; phenanthrene, 85-01-8; diphenylmethanol, 91-01-0; benzophenone, 119-61-9; anthracene, 120-12-7.

(43) Weitz, E.; Vollmer, W. *Ber.* **1924**, *57B*, 1015-1018.
(44) Scott, A. W. *J. Am. Chem. Soc.* **1927**, *49*, 986-987.
(45) Polydoropoulos, C. N. *Chem. Ind. (London)* **1963**, 1686.

Laser Raman and Infrared Spectra, and X-ray Crystal Structure of *trans*-Di-*tert*-butyl Hyponitrite

Craig A. Ogle,*[1a] Karen A. VanderKooi,[1b] G. David Mendenhall,*[1b] Veerayooth Lorprayoon,[1b] and Bahne C. Cornilsen*[1b]

Contribution from the Department of Chemistry, University of Arizona, Tucson, Arizona 85721, and the Department of Chemistry and Chemical Engineering, Michigan Technological University, Houghton, Michigan 49931. *Received January 28, 1982*

Abstract: The molecular structure of *trans*-di-*tert*-butyl hyponitrite has been determined from a single-crystal, low-temperature X-ray study. The compound crystallizes in a monoclinic space group $P2_1/c$ with two molecules per unit cell. The molecule has N=N, N—O, and O—C distances of 1.252 (5), 1.380 (6), and 1.471 (7) Å, respectively, and an N=N—O angle of 106.5 (3)°. The IR and Raman band assignments were made with the aid of $^{15}N/^{14}N$ isotopic substitution. The Raman spectra allowed unique assignment of the ν_{NO} and ν_{CO} stretching modes. These overlap in the ^{14}N spectrum to give the characteristic, IR-active band at 990 cm^{-1}. The Raman active $\nu_{N=N}$ is assigned at 1509 cm^{-1}.

Introduction

Alkyl hyponitrites have been known for a number of years as useful, low-temperature sources of alkoxy radicals.[2] A number of very significant studies of solvent and pressure effects on cage recombination[3] and of free-radical chain oxidations[4] and polymerizations[5] have been carried out with di-*tert*-butyl or dicumyl hyponitrites. The total literature on hyponitrites is sparse, however, as compared with the literature on the closely related azoalkanes.

Although the crystal structures of some interesting cis[6] and trans[7] organometallic hyponitrites have been determined, the trans geometries of the simple alkyl derivatives have only been inferred on the basis of the vibrational spectra of sodium[8] and silver[8a] hyponitrites from which the organic hyponitrites were synthesized. A study of the dipole moments of two alkyl hyponitrites also supported the trans structure.[9]

We now report the X-ray crystal structure of an organic hyponitrite for the first time. The IR and Raman vibrational spectra are assigned using $^{15}N/^{14}N$ isotopic substitution, and the results are completely consistent with the space group and trans structure found in the single crystal analysis. Solution ($CHCl_3$) and solid-state Raman spectra are similar and indicative of the trans structure.

Experimental Section

X-ray Study. Colorless, transparent, rectangular parallelepiped crystals of di-*tert*-butyl hyponitrite were obtained from pentane solution upon cooling. The compound was prepared by Traylor's procedure from silver hyponitrite and *tert*-butyl bromide.[2c] A 250-MHz ^1H NMR scan of the product in $CDCl_3$ gave no indication of major impurities or isomers.

X-ray diffraction data were collected with a computer-controlled Syntex $P2_1$ four-circle diffractometer [Mo Kα ($\bar{\lambda}$ = 0.71073 Å)] at −50 °C. Initially 25 reflections (range $6° \le 2\theta \le 31°$) were used to calculate cell constants. Axial photographs and systematic absences in the 1045 reflections indicated the monoclinic space group $P2_1/c$ with $Z = 2$. Final cell parameters were a = 5.739 (2), b = 10.870 (5), c = 8.762 (4) Å, β = 108.13 (3)°, corresponding to a cell volume of 524.0 (4) Å^3. The calculated density, 1.10 g/cm^3, and the measured density, 1.05 (4) g/cm^3

(1) (a) University of Arizona. Address inquiries to Institut de Chimie Organique de l'Université, Rue de la Barre 2, CH-1005, Lausanne, Switzerland. (b) Michigan Technological University.
(2) (a) Hughes, M. N. *Q. Rev., Chem. Soc.* **1968**, *22*, 1-13. (b) deSousa, J. B. *Nature (London)* **1963**, *199*, 64-5. (c) Kiefer, H.; Traylor, T. G. *Tetrahedron Lett.* **1966**, 6163-8.
(3) (a) Kiefer, H.; Traylor, T. G. *J. Am. Chem. Soc.* **1967**, *89*, 6667-71. (b) Dulog, L.; Klein, P. *Chem. Ber.*, **1971**, *104*, 902-8. (c) Neuman, R. C., Jr. *J. Org. Chem.* **1972**, *37*, 495-6. (d) Neumann, R. C., Jr.; Bussey, R. J. *J. Am. Chem. Soc.* **1970**, *92*, 2440-5. (e) Neumann, W. P.; Lind, H. *Chem. Ber.* **1968**, *101*, 2837-44.
(4) (a) Howard, J. A.; Ingold, K. U. *Can. J. Chem.* **1969**, *47*, 3797-801. (b) Dulog, L.; Klein, P. *Chem. Ber.* **1971**, *104*, 895-901. (c) Barclay, L. R. C.; Ingold, K. U. *J. Am. Chem. Soc.* **1981**, *103*, 6478-85.
(5) (a) Ray, N. H. *J. Chem. Soc.* **1960**, 4023-8. (b) Marshall, I.; Harris, I.; Garrett, K. B. British Patent 618 168, 1949; *Chem. Abstr.* **1949**, *43*, 5641. (c) Batty, J. W.; Lambert, A.; Scott, G.; Seed, L. British Patent 813 460, 1959; *Chem. Abstr.* **1959**, *53*, 19877. Numerous other patents on hyponitrite initiators have appeared.
(6) (a) Hoskins, B. F.; Whillans, F. D.; Dale, D. H.; Hodgkin, D. C. *Chem. Commun.* **1969**, 69-70. (b) Bhaduri, S.; Johnson, B. F. G.; Pickard, A.; Raithby, P. R.; Sheldrick, G. M.; Zuccaro, C. I. *J. Chem. Soc., Chem. Commun.* **1977**, 354-5.
(7) Bau, R.; Sabherwal, I. H.; Burg, A. B. *J. Am. Chem. Soc.* **1971**, *93*, 4926-8.
(8) (a) Kuhn, L.; Lippincott, E. R. *J. Am. Chem. Soc.* **1956**, *78*, 1820-1. (b) Millen, D. J.; Polydoropoulos, C. N.; Watson, D. *J. Chem. Soc.* **1960**, 687-91. (c) Goubeau, J.; Laitenberger, K. *Z. Anorg. Allg. Chem.* **1963**, *320*, 78-85.
(9) Hunter, E. C. E.; Partington, J. R. *J. Chem. Soc.* **1933**, 309-313.

0002-7863/82/1504-5114$01.25/0

(average of two measurements by flotation method with H_2O/NaI), were in good agreement considering the different experimental temperatures.

During data collection three test reflections at the three angles of most intense reflection were made every 22 data points. These check reflections showed less than 2% change, indicating little decomposition of the crystal by the incident X-ray beam. A θ–2θ scan over the range $4° \leq 2\theta \leq 50°$ was used to collect a total of 1045 unique reflections. Of these, 497 having $I \geq 3\sigma(I)$ were used to solve and refine the structure.

Direct methods[10] were used with MULTAN 78[11] and the 250 largest E's to solve the structure. The positions of all nonhydrogen atoms were obtained from an "E-map" based on the solutions with the highest combined figure of merit. The structure was refined by full-matrix least-squares techniques.[12] Refinement of the structure was initiated with neutral atom scattering factors for all species.[13] The structural parameters for the nonhydrogen atoms were first refined isotropically to convergence ($R = 0.1198$ and $R_w = 0.1481$) and then refined anisotropically to convergence ($R = 0.1057$ and $R_w = 0.1349$). A hydrogen on each methyl was located from structure factor calculations and a difference electron density map. The other hydrogen positions were calculated assuming tetrahedral geometry and standard C–H bond lengths, and assigned temperature factors according to $B_H = B_N$, where N is the atom to which H is bonded. Hydrogen parameters were not refined. The nonhydrogens were then further refined anisotropically to convergence ($R = 0.0595$ and $R_w = 0.0661$). The largest residual peak in the final electron density difference map was 0.31 e/Å^3, indicating the absence of solvent of crystallization. Thermal parameters for the atoms are available upon request from G.D.M. or C.A.O.

Laser Raman Spectroscopy. Raman spectra were scanned on samples in glass capillaries (1.5-mm i.d.) using an Instruments S.A. Model HG.2S, four-slit double monochromator. Low laser intensities (≤100 mW) were used to avoid decomposition. Multiple scan, signal-averaged spectra were collected with a Tracor Northern NS-570A signal averager. This was interfaced to a Nova 3/12 minicomputer via a Tracor Northern NS-441A interface. A scan rate of 20 cm^{-1}/min was used with both 1 and 4 cm^{-1} slit widths. Data were collected at 0.5 and 1.0 wavenumber increments, respectively. Three scans were averaged for the spectrum with 1 cm^{-1} slit width. Laser plasma lines and a mercury-vapor lamp were used for calibration. Incident laser lines at 488.0 nm and 514.5 nm from a Coherent model CR-4 argon ion laser were used to confirm that the observed spectra were Raman scattered.

Infrared Spectroscopy. Conventional KBr pellets were prepared in the usual way containing about 1% of organic sample. The spectra were recorded on a Perkin-Elmer Model 621 or a Beckman Model 4240. Polystyrene film was used for calibration.

***tert*-Butyl Hyponitrite-$^{15}N_2$.** This compound was prepared in the conventional way[2c] from sodium and silver hyponitrite-$^{15}N_2$ and crystallized once from methanol at −20 °C, giving white needles which were collected by centrifugation. The $Na_2{}^{15}N_2O_2$ was prepared in the following manner. Two sidearm test tubes and a bubbler were connected with glass and Tygon^R tubing so that gas passed to the bottom of the first tube to the bottom of the second and then to the bubbler. Both tubes contained small magnetic stirring bars, and a small drying tube with nonindicating $CaSO_4$ was connected between them. The first tube (20 × 150 mm) was charged with 0.46 g (6.6 mmol) of $Na^{15}NO_2$ (99% isotopic purity, Prochem), 2.8 g (6.6 mmol) of potassium ferrocyanide (Mallinckrodt), and water (6.4 mL). The second tube (25 × 200 mm) contained 0.35 g (15 mmol) of sodium sand, toluene (4 mL), benzophenone (3.3 g, 18 mmol), and 1,2-dimethoxyethane (14 mL, Fisher) under nitrogen. The first tube and the drying tube were swept with N_2 before being attached to the second tube and bubbler. The N_2 flow was reduced to about 1 bubble/s, the contents of the tubes were stirred, and the reaction was initiated by injecting acetic acid (0.8 mL) through the tubing into the first test tube. After 1 h the contents of the second tube was quenched with water (1 mL) under N_2 (CAUTION) and worked up as described elsewhere.[14] The yield of crude white solid was 0.20 g. The EI mass spectrum (Hewlett-Packard Model 5985) of *tert*-butyl hyponitrite-$^{15}N_2$ showed major signals at m/e 176 and 145, in addition to alkyl contributions at 57, 43, 41, and 39 which were also present in spectra of unenriched samples. The relative intensities of the signals at m/e 175–7, after correction for some self-protonation, allowed us to determine the isotopic purity as 99.1%.

Di-*tert*-butyl peroxide (Shell) was purified by passage through a short column of alumina and then distilled by the bulb-to-bulb technique.

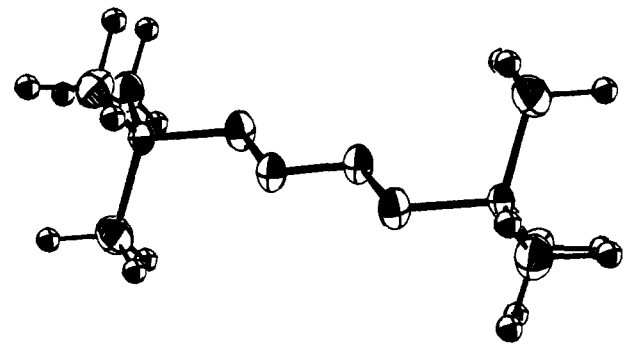

Figure 1. ORTEP perspective view of di-*tert*-butyl hyponitrite. The hydrogen atoms have been assigned arbitrary thermal parameters. Thermal ellipsoids drawn to enclose 50% of the probability distribution.

Table I. Bond Distances and Angles for *trans*-Di-*tert*-butyl Hyponitrite

bond	distance, Å	group	angle, deg
N=N	1.252 (6)	N=N–O	106.5 (3)
N–O	1.380 (6)	N–O–C(1)	109.3 (3)
O–C(1)	1.471 (7)	O–C(1)–C(2)	101.3 (3)
C(1)–C(2)	1.523 (7)	O–C(1)–C(3)	110.1 (3)
C(1)–C(3)	1.486 (6)	O–C(1)–C(4)	109.7 (3)
C(1)–C(4)	1.506 (8)	C(2)–C(1)–C(3)	112.1 (4)
		C(2)–C(1)–C(4)	110.6 (4)
		C(3)–C(1)–C(4)	112.5 (4)

Table II. Bond Lengths and Distances for Some Azo Compounds

R in *trans*-RN=NR	N=N, Å	angle NNX, deg	ref	$\nu^s_{N=N}$, cm^{-1}	ref
H	1.238 (7)	109 (1.5)	*a*	1529	*f*
F	1.230 (1)	105.5 (0.7)	*b*	1522	*g*
t-BuO	1.252 (6)	106.5 (0.3)	this work	1509	this work
Me	1.254 (3)	111.9 (0.5)	*c*	1576 (neat)	*h*
Ph	1.243 (3) 1.172 (3)	113.5 (0.2) 111.1 (0.2)	*d*	1442	*h*
$Me_2C(CN)$	1.223 (4) 1.217 (3)	114.2 (0.2) 114.8 (0.2)	*e*	1580	*h*
CH_3, CF_3	1.219 (8)		*c*	1592 (IR)	*i*

[a] Trombetti, A. *Can. J. Phys.* 1968, *46*, 1005–11. [b] Bohn, R. K.; Bauer, S. H. *Inorg. Chem.* 1967, *6*, 309–12. [c] Chang, C. H.; Porter, R. F.; Bauer S. H. *J. Am. Chem. Soc.* 1970, *92*, 5313–8. [d] Brown, C. J. *Acta Crystallogr. Sect. A* 1966, *21*, 146–52. Two nonequivalent sites occur in the unit cell. [e] Jaffe, A. B.; Malament, D. S.; Slisz, E. P.; McBride, J. M. *J. Am. Chem. Soc.* 1972, *94*, 8515–8521. Data are for two crystal modifications. [f] Bondybey, V. E.; Nibler, J. W. *J. Chem. Phys.* 1973, *58*, 2125–34. [g] Reference 22. [h] Reference 19, p 331. [i] Dinwoodie, A. H.; Haszeldine, R. N. *J. Chem. Soc.* 1965, 2266–8.

Results and Discussion

Crystal Structure. The bond distances and angles for *trans*-di-*tert*-butyl hyponitrite (Figure 1) in Table I show expected values for the familar groups. There is a substantial decrease in the O–C(1)–C(2) angle from the tetrahedral value, and a rather long bond between C(1) and C(2). The O–C(1) distance, however, is comparable to that in methyl nitrite[15] (1.44 ± 0.02 Å), and the N–O distance comparable to that in formaldoxime[16] (1.408 Å)

(10) All computations were performed on the CDC CYBER-175 computer at the University of Arizona computer center.

(11) Germain, G.; Main, P.; Woolfson, M. M. *Acta Crystallogr. Sect. A* **1971**, *27*, 368–76.

(12) The major programs used during the structure determinations were FORDAP (Fourier summation program by A. Zalkin) and NUCLS (structure factor calculations and full-matrix least-squares refinement by J. Ibers, itself a modification of ORFLS, by W. Busing, K. Martin, and H. Levy).

(13) Scattering factors were obtained from "International Tables for X-Ray Crystallography", Kynoch Press: Birmingham, England, 1974; Vol. IV, pp 71–98.

(14) Mendenhall, G. D. *J. Am. Chem. Soc.* **1974**, *96*, 5000. See cautionary note in accompanying paper: Mendenhall, G. D., et al. *Ibid.*, preceding paper in this issue.

(15) Rogowski, F. *Ber.* **1942**, *75*, 244–69.

Table III. Results of Point Group and Factor Group Analyses[a]

	symmetry species				activity	
	A_g	B_g	A_u	B_u	Raman	IR
internal modes						
C_{2h} free molecule group	24	18	19	23	42	42
C_i site group	42	0	42	0	42	42
C_{2h} factor group	42	42	42	42	84	84
external modes						
rotations	3	3	0	0	6	0
translations	0	0	2	1	0	3
acoustic	0	0	1	2	0	0
total no.						
of active species	45	45	44	43	90	87
(in solution)	(25)	(20)	(20)	(25)	(45)	(45)

[a] None of the Raman and infrared bands are coincident.

and methyl nitrite[15] (1.37 ± 0.02 Å). The N-O-C(1) angle is virtually identical with the corresponding angle in methyl nitrite[15] (109.5°).

Häfelinger[17] has presented simple linear equations which relate a π bond-order parameter p_{rs} to bond lengths in a number of types of nitrogen compounds. With the data from Table I we calculate by his method, $p_{rs} = 0.90$ for the N=N bond and $p_{rs} = 0.25$ for the N—O bond. The former is reasonable, and the latter comparable to $p_{rs} = 0.17$–0.20 calculated for the N–O bond in formaldoxime.

Comparison of a series of trans-azo compounds (Table II) shows that the N=N bond is nearly constant at 1.23 ± 0.02 Å, and that the N=N—X bond angle decreases as X becomes more electronegative. The angle in the hyponitrite is most similar to that in *trans*-N_2F_2. This is interesting because *cis*-N_2F_2 is thermodynamically more stable.[18]

Vibrational Spectra. Factor Group Analysis. A complete set of vibrational modes for the unit cell is predicted by a factor group analysis (fga). All the atoms are on C_1 sites which each contain four equivalent atoms. There are 15 atoms (one-half of a molecule, $(CH_3)_3CON$) per asymmetric unit which are related by the fourfold unit cell symmetry (or equivalency). Correlation of the three translations (3A species of the C_1 site group) for each atom with the C_{2h} factor group gives $45A_g + 45B_g + 44A_u + 43B_u$ modes after subtraction of the acoustic modes ($A_u + 2B_u$). The internal modes are correlated with the $3n - 6$ molecular vibrations for one molecule through a C_i molecular site (see Figure 1 for structure):

C_{2h} free molecule species	C_i site species	C_{2h} factor group species
A_g or B_g	A_g	A_g
		B_g
A_u or B_u	A_u	A_u
		B_u

Note that each molecular species is split by the factor group effect. However, no infrared band (A_u or B_u) becomes Raman active and no Raman band (A_g or B_g) becomes infrared active in the factor group. Table III summarizes these results.

It is in principle necessary to classify the vibrational species predicted on the full unit cell basis (see Table III); however, based upon the factor group analysis it can be seen that two simplifying approximations, which are empirically substantiated, allow empirical band assignments for all major infrared and Raman bands. These approximations are (a) that factor group splitting of each infrared band (u–u splitting) and each Raman band (g–g splitting) is not observable or not resolvable, and (b) that the *tert*-butyl modes of similar symmetry do not couple in a complex manner; rather it is possible to categorize them collectively in terms of "*tert*-butyl group frequencies".[19] To provide skeletal structural information it is necessary to differentiate the *tert*-butyl modes from the skeletal modes.

Table IV. Skeletal Mode Assignments and $^{14}N/^{15}N$ Isotopic Shifts for Solid-State Spectra

Raman spectrum[a]	infrared spectrum[a]	isotopic shift[b]	band assignment
1509		40	ν^s_{NN} (A_g)
1067		17	$\nu^s_{NO} + \nu^s_{CO}$ (A_g)
1028		13	$\nu^s_{CO} + \nu^s_{NO}$ (A_g)
	990	~10	ν^a_{NO} (B_u) / ν^a_{CO} (B_u)
	594	6	δ^a_{NNO} (B_u)
583		3	δ^s_{NNO} (A_g)
494		~1	δ^s_{NOC} (A_g)
	476	<2	δ^a_{NOC} (B_u)
	?	?	δ^a_{NOCC}(oop) (A_u)
184		≤1	δ^s_{NOCC}(oop) (B_g)
	?	?	δ^a_{NNOC}(oop) (A_u)
165		3	δ^s_{NNOC}(oop) (B_g)
	?	?	δ^a_{ONNO}(oop) (A_u)

[a] ^{14}N wavenumbers listed. [b] $\Delta\tilde{\nu} = \tilde{\nu}(^{14}N) - \tilde{\nu}(^{15}N)$.

Solid-state effects (i.e., factor group effects) can complicate spectral analysis and make it difficult or impossible to distinguish cis vs. trans structures. The factor group analysis shows that this potential complication does not arise for this unit cell. The molecular vibrations fully reflect the trans vs. cis structure. The solid-state splitting predicted by the FGA does not relax this result of the mutual exclusion principle.

Because of the center of symmetry and invocation of the mutual exclusion principle, the noncoincident Raman and infrared spectra will each, at first approximation, look like that of an individual $(CH_3)_3CON$ group. The g–u splitting between the Raman and infrared bands is proportional to the extent of coupling between the similar vibrations on either side of the center of symmetry. In addition to these vibrations, an N–N stretch, ν_{NN}, and an ONNO out-of-plane bend, δ_{ONNO}, are expected in the Raman spectrum and the infrared spectrum, respectively.

Isotopic Substitution and Band Assignment of Skeletal Modes. For a trans (C_{2h}) hyponitrite one expects nine stretching and bending skeletal (CONNOC) modes, five Raman-active and four IR-active. None of these is predicted to be mutually infrared and Raman active on the basis of the trans molecular model. These modes include ν^s_{NN} plus symmetric and asymmetric pairs for ν_{NO}, ν_{CO}, δ_{NNO}, and δ_{NOC}.

Upon isotopic substitution, eight bands are observed to shift (Figure 2 and Table IV) in the spectral region in which skeletal vibrations are expected (400 to 1600 cm^{-1}) and must involve nitrogen atom motion. None of the bands that shift possesses a coincident band in the other spectrum; e.g., the 583-cm^{-1} Raman-active mode has no counterpart in the IR spectrum. The five Raman active modes that shift are each fully polarized in $CHCl_3$ solution, confirming A_g symmetry.

The 1509-cm^{-1} Raman band shifts 40 cm^{-1} with isotopic substitution and is a very intense Raman band. This is assigned to the symmetric N–N stretch, ν^s_{NN}, mode. In other azo compounds this mode appears between 1600 and 1440 cm^{-1} (Table II). No asymmetric N–N stretch is predicted nor seen in the infrared spectrum. The latter would be active for a cis compound.

With ^{15}N substitution, the 1067-cm^{-1} band shifts to 1050 cm^{-1}, and the 1028-cm^{-1} band shifts to 1015 cm^{-1}. These two bands are assigned as the ν^s_{NO} and ν^s_{CO} stretching modes, respectively. The ν_{CO} mode will experience an isotope shift only if coupled to the ν_{NO} mode, and this is indeed observed. The band which shifts more (17 cm^{-1}) probably reflects the greater amount of N-O stretching character. Upon isotopic substitution, the 1028-cm^{-1} band shifts to reveal a weaker band at 1027 cm^{-1}. The shoulder

(16) Levine, I. N. *J. Chem. Phys.* **1963**, *38*, 2327–8.
(17) Häfelinger, G. *Chem. Ber.* **1970**, *103*, 3370–3392.
(18) Armstrong, G. T.; Marantz, S. *J. Chem. Phys.* **1963**, *38*, 169–72.
(19) (a) Dollish, F. R.; Fateley, W. G.; Bentley, F. F. "Characteristic Raman Frequencies of Organic Compounds"; Wiley: New York, 1974; pp 4–6. (b) Colthup, N. B.; Daly, L. H.; Wiberley, S. E. "Introduction to Infrared and Raman Spectroscopy"; Academic Press: New York, 1975; pp 220–227. (c) *Ibid.* p 225.

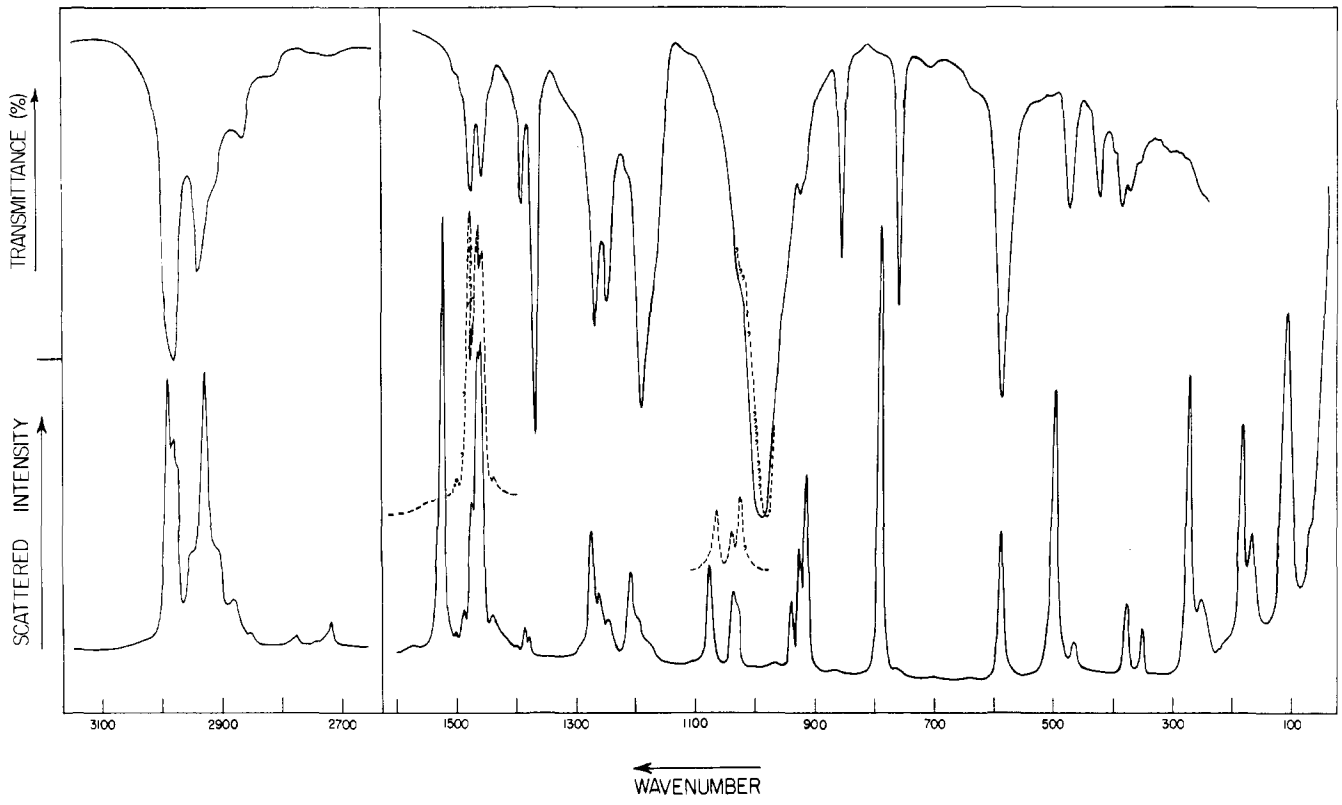

Figure 2. Infrared (top) and Raman (bottom) spectra of *tert*-butyl hyponitrite. The significant shifts in the spectra of the N-15 substituted hyponitrite are shown as dotted lines.

at 1025 cm^{-1} apparently remains in this region. It is not observed in the ^{15}N spectrum but may be buried in the 1027–1015-cm^{-1} overlap region.

A broad IR band at 990 cm^{-1} shifts to 980 cm^{-1} in the IR spectrum of ^{15}N-substituted hyponitrite. The resolution of the two coupled Raman bands, ν^s_{CO} and ν^s_{NO}, with ^{15}N substitution supports assignment of ν^a_{CO} and ν^a_{NO} for this broad 990-cm^{-1} infrared band. These two asymmetric stretches are not resolved in the infrared spectrum, although the band broadens with ^{15}N substitution. For comparison, the symmetrical C–O–C stretching mode in vinyl ethers[20] typically occurs at 1075–1020 cm^{-1}, and the C–O stretch in alkyl nitrites, at 1045–993 cm^{-1}.[21] The N–O stretching mode in alkyl nitrites occurs at 850–750 cm^{-1}.[21] In $N_2O_2^{2-}$ the N–O stretching modes are assigned at 1121–830 cm^{-1}.[22]

A lower energy infrared band at 594 cm^{-1} shifts 6 cm^{-1} upon ^{15}N substitution and is near a Raman band at 583 cm^{-1} which shifts 3 cm^{-1}. A lower energy pair at 494 and 476 cm^{-1} demonstrates very small isotopic shifts (≤ 2 cm^{-1}). Both Raman bands are polarized. These two pair are assigned to the NNO and NOC symmetric and asymmetric bends. The first pair exhibits larger isotopic shifts and is tentatively assigned as the symmetric and asymmetric NNO bending modes.[23]

Finally, three out-of-plane (oop) bends are predicted for this CONNOC skeleton. A low-energy Raman band at 165 cm^{-1} shifts with isotopic substitution and can be assigned as an NNOC or an NOCC oop bend. The second Raman-active oop bend cannot be definitely assigned since no other isotopic shifts are observed, and is tentatively assigned to the 184-cm^{-1} Raman band. The CCOO torsion in di-*tert*-butyl peroxide has been assigned to a 242-cm^{-1} band.[24] The third infrared active oop bend, δ_{ONNO}, has not been observed and probably appears below 250 cm^{-1}.

Alkyl Band Assignments. The *tert*-butyl mode assignments are summarized in Table V. The Raman modes consist of two triplets in the CH stretching region, five triplets (deformation and rocking modes) and three C–C stretches between 1500 and 700 cm^{-1}, five OCC_3 rock and deformation modes below 500 cm^{-1}, and methyl and *tert*-butyl torsions below 300 cm^{-1}. Corresponding bands appear in the infrared spectrum, although they are broader and less resolvable. The literature defines characteristic *tert*-butyl group bands found in each of several regions denoted with an asterisk in Table V (refer to set A).[19] The spectra for various *tert*-butyl compounds do differ between 1300 and 800 cm^{-1} which allows significant variation in assignments for bands in this region (δ_{CH_3}, ρ_{CH_3}, and ν_{CC}).

C–H Stretching Region. The Raman bands in the C–H stretching region are assigned (Table V) at 2986 (asymmetric) and 2930 cm^{-1} (symmetric) in solution. The 2950- and 2908-cm^{-1} bands may be the second and third components of a triplet ν^s_{CH}. These bands are also present in the solid-state Raman spectrum and may result from coupling of the three totally symmetric C–H stretching vibrations (one per methyl group).[19c] The weaker asymmetric stretch at 2986 cm^{-1} increases in intensity and splits into three modes in the solid spectrum at 2992, 2986, and 2980 cm^{-1}. This splitting is apparently the result of three nonequivalent methyls which are no longer free to rotate in the solid. Such intensity enhancement for ν^a_{CH} modes has been reported in solid-state infrared spectra.[19c] This was ascribed to an increase in dipole moment (μ) as free rotation was hindered. The mechanism apparently has a similar influence upon the polarizability tensor (α) of ν^a_{CH} in the Raman spectrum of this compound. We propose that this is related to the formation of a more ordered *tert*-butyl group in the solid. This ordering leads to *both* greater splitting of the ν^a_{CH} triplet and an increase in intensity as both μ and α are influenced. The splitting is determined by the coupling of the six methyl groups (g–u, u–u, and g–g) under the C_i site symmetry.

The infrared-active C–H stretching modes parallel the Raman bands in intensity and approximate position. Although the infrared bands are broad and overlapped, it is evident that the infrared and Raman bands are noncoincident. They are summarized in

(20) Silverstein, R. M.; Bassler, G. C.; Morrill, T. C. "Spectrometric Identification of Organic Compounds", 4th ed.; Wiley: New York, 1981; p 116.
(21) Tarte, P. *J. Chem. Phys.* **1952**, *20*, 1570–75.
(22) Ross, S. D. "Inorganic Infrared and Raman Spectra"; McGraw Hill: London, 1972; pp 169–70.
(23) We observe analogous bands in the Raman spectrum of *tert*-butyl nitrite at 581 (δ_{ONO}) and 491 cm^{-1} (δ_{NOC}).

Table V. Vibrational Mode Assignments

Raman spectra		infrared	band assignments	
solution[a]	solid	solid	set A	set B
	2992 vs			
2985 m	2986 s	2983 vs, brd	ν^{a}_{CH}	$3A_g + 3B_g + 3B_u + 3A_u$
	2980 s, sh			
2950 sh	2956 sh			
		2940 m		
2930 s (sP)	2933 s		ν^{s}_{CH}	$2A_g + B_g + 2B_u + A_u$
		2918 sh		
2908 m	2910 w, sh			
2882 m	2884 w			
		2873 w		
2854 w, sh	2858 w, sh		overtone and	
2778 w	2778 w		combination	
2722 mw	2722 w		bands	
1512 vs (P)	1509 vs			ν^{s}_{NN} (A_g)
	1474 vw	1479 m	$\delta^{a}_{CH_3}$	
1459 ms (P)	1461 m, sh	1461 m		$\delta^{s}_{CH_3}$
	1452 s			
1447 s (dp)	1447 s		$\delta^{a}_{CH_3}$[b]	
	1425 vw			
1369 w (P?)	1373 w	1393 m	$\delta^{s}_{CH_3}$[b]	$\delta^{a}_{CH_3}$
1336 w (P)	1365 w	1369 s		
1263 m (dp)	1262 m	1270 ms		
1253 sh[c]	1252 sh	1250 ms	$\rho_{CH_3} + \nu_{CC}$[b]	$\delta^{a}_{CH_3}$
c	1234 sh			
c	1198 m	1190 s		
c	1174 sh		$\nu_{CC} + \rho_{CH_3}$[b]	$\rho^{a}_{CH_3}$ (+ skeletal?)
c	1168 sh			
1070 m (sP)	1067 m		skeletal	$\nu^{s}_{NO} + \nu^{s}_{CO}$ (A_g)
1025 m (P)	1028 m		skeletal	$\nu^{s}_{CO} + \nu^{s}_{NO}$ (A_g)
		1030 sh	e	ν^{a}_{CC} (A_u)
	1027 w[f]		e	ν^{s}_{CC} (A_g)
	1025 sh		e	ν^{s}_{CC} (B_g)
		990 vs, brd	skeletal	ν^{a}_{NO} (B_u)
				ν^{a}_{CO} (B_u)
929 s (P)	931 s	927 w		
919 m (P)	918 m		ρ_{CH_3}	$\rho^{s}_{CH_3}$
906 m (P)	907 m			
	~861 vw	860 ms		ν^{a}_{CC} (B_u)
784 vs (sP)	786 vs		ν^{s}_{CC}[b]	$\nu^{s}_{CC_3}$ (A_g)
	~756 vw	760 s		ν^{a}_{CC} (B_u)
		594 s		δ^{a}_{NNO} (B_u)
587 s (sP)	583 m			δ^{s}_{NNO} (A_g)
495 vs (sP)	494 s			δ^{s}_{NOC} (A_g)
		476 m		δ^{a}_{NOC} (B_u)
c	462 w			$\delta^{s}_{CC_3}$ (B_g)
		423 m		$\delta^{a}_{CC_3}$ (B_u)
		388 w	δ_{CCC}[b]	$\delta^{s}_{CC_3}$ (A_u)
c	376 w	377 w	and δ_{OCC}	$\delta^{s}_{CC_3}$ (A_g)
c	350 w			ρ_{CC_3} (A_g or B_g)
c	272 s	d	ρ_{CC_3}[b]	τ_{CH_3} (A_g)
c	248 w			τ_{CH_3} (B_g)
181 s	184 s			δ^{s}_{NOCC} (B_g)
c	165 m			δ^{s}_{NNOC} (B_g)
	108 s			

[a] P = polarized, sP = strongly polarized ($\rho_\perp/\rho_\parallel < 20\%$), dp = depolarized. [b] Characteristic *tert*-butyl group vibrational mode.[19] [c] Obscured by $CHCl_3$ solvent bands. [d] Infrared scanned from 250 to 4000 cm^{-1}. [e] Unassigned in set A (see text). [f] Revealed upon ^{15}N substitution.

Table V. Weaker bands between 2900 and 2700 cm^{-1} in both the infrared and Raman spectra are probably overtone and combination bands.[19b]

Assignment of δ_{CH_3}, ρ_{CH_3}, and ν_{CC}. Each methyl group displays three deformation and two rocking modes. For each type, rock or deformation, there will be a triplet resulting from coupling of the three methyls of a *tert*-butyl group. For the di-*tert*-butyl molecule the two groups, therefore, produce 30 bands. Fifteen are Raman active (the two *tert*-butyl groups are vibrating in phase, g-type modes) and 15 are infrared active (the two end groups are vibrating out-of-phase, u modes). Each rock (ρ) or deformation (δ) is expected to consist of a triplet unless unresolved or coupled with other vibrations. Assignment of the rocking modes is commonly complicated by coupling with *tert*-butyl skeletal modes, ν_{CC}.[19,24,25] Rocking modes couple with δ_{COH} modes in *tert*-butyl alcohol.[26]

The totally symmetric *tert*-butyl skeletal mode, $\nu^{s}_{CC_3}$, is expected to be very strong in the Raman spectrum and polarized; it is assigned to the intense band at 785 cm^{-1}. Two strong infrared

(24) McKean, D. C.; Duncan, J. L.; Hay, R. K. M. *Spectrochim. Acta, Part A* **1967**, *23*, 605.
(25) Bertie, J. E.; Sunder, S. *Can. J. Chem.* **1973**, *51*, 3344–53.
(26) Pritchard, J. G.; Nelson, H. M. *J. Phys. Chem.* **1960**, *64*, 795–801.

modes at 860 and 760 cm^{-1} flank this peak and are assigned to ν_{CC} modes. The spectra of di-*tert*-butyl peroxide contain three analogous bands.[24] The two ν_{CC} modes of lower symmetry, A_g and B_g, split from an E mode for a C_{3v} *tert*-butyl group, remain to be assigned as does the third infrared-active ν_{CC} mode (A_u or B_u species). Whether these *remaining* unassigned ν_{CC} modes couple with ρ_{CH_3} modes or not can be questioned. Coupling of triplet ρ_{CH_3} modes with ν_{CC} would be expected to break up the triplet pattern. One or two, but not all three bands of a triplet could couple with the A_g and B_g, ν_{CC}, modes. However, three or four sets of triplets are observed in the Raman spectrum with no obvious disruption.

Whether one applies such coupling in assigning vibrational modes in the 1600- to 800-cm^{-1} region or not, there are complications. As mentioned above, five *sets* of methyl vibrations are expected in this region, three deformations and two rocking modes. The deformations are generally assigned between 1500 and 1350 cm^{-1} (see Table V, assignment "set A"). If we assign the two rocks at ca. 907 (referring to each triplet by the most intense band) and ca. 1262 cm^{-1}, several bands are left unassigned. The latter include a triplet at ca. 1197 and a doublet at 1027 cm^{-1}. These are not accounted for by the *two* remaining ν_{CC} assignments.

Because of these difficulties, two different sets of *tert*-butyl assignments (A and B) are given in Table V. The above set of assignments, designated as set A of Table V, is consistent with the traditional *tert*-butyl assignments found in the literature.[24-26]

The second set of *tert*-butyl assignments (Table V, set B) does not require coupling of methyl rock and C–C stretching vibrations. One methyl deformation, δ_{CH_3}, is assigned in the 1300- to 1200-cm^{-1} region to the ca. 1262-cm^{-1} Raman triplet and an infrared doublet, 1250 and 1270 cm^{-1}. This is somewhat lower in energy than is usual for alkanes. The two remaining ν^s_{CC} modes are assigned to bands at 1027 cm^{-1} (uncovered upon isotopic substitution) and 1025 cm^{-1} (^{14}N spectrum). The 1027-cm^{-1} band does not couple to the ν_{NO} and ν_{CO} modes since there is no definite shift upon ^{15}N substitution. The 1027-cm^{-1} band and 1025-cm^{-1} shoulder in the Raman spectrum of the hyponitrite correspond to a pair of bands at 1041 and 1022 cm^{-1} in the Raman spectrum of *tert*-butyl peroxide. The latter were not assigned.[24] We ascribe these to nontotally symmetric CC stretching modes as well. The third infrared-active ν^a_{CC} is tentatively assigned to the 1030-cm^{-1} shoulder. It becomes more prominent as the 990-cm^{-1} band shifts to 980 cm^{-1} with ^{15}N substitution. A similar band is observed in this region in other *tert*-butyl spectra.[24-26]

The latter set B assignments clearly designate four sets of triplets in the Raman spectrum as methyl bending modes. The symmetric and asymmetric C–H stretches form triplets as mentioned above. The spectra can therefore be assigned without resort to ρ_{CH_3}–ν_{CC} coupling arguments. A small isotopic shift at 1198 cm^{-1} (≤ 2 cm^{-1}), however, appears to be real and would suggest some coupling of this $\rho^a_{CH_3}$ to a mode involving nitrogen motion. This could imply skeletal character in accord with assignments of set A.

Weak bands at 1474 and 1425 cm^{-1} may be overtone or combination modes. Solid-state splitting does not explain their appearance since they exist in solution as well.

Assignment of δ_{CC_3}, ρ_{CC_3}, and τ_{CH_3}. These modes (see Table V) are ascribed to bands between 462 and 248 cm^{-1} by direct analogy with the assignments made by Durig et al. for a series of *tert*-butyl derivatives.[27] The band at 108 cm^{-1} may be assigned to an external, lattice mode.

Conclusions

The X-ray data conclusively show that the common form of *tert*-butyl hyponitrite has the trans structure. This information and isotopic substitution allows assignment of characteristic ν_{NN}, ν_{NO}, and ν_{CO} modes, together with related bending modes. The skeletal mode assignments demonstrate mutual exclusion, consistent with the trans structure in both solid-state and solution spectra. The vibrational bands of *tert*-butyl origin have also been assigned. Infrared-Raman u–g splitting varies from 77 cm^{-1} for skeletal modes to <10 cm^{-1} for the more remote *tert*-butyl modes. Similarities between other *tert*-butyl spectra and those reported herein suggest that it may be misleading to interpret spectra in terms of E modes and assumed C_{3v} symmetry.

Acknowledgment. The authors wish to thank Drs. J. H. Enemark and W. N. Setzer for assistance with the X-ray determination, Mr. Jim Knight for use of the IR facilities at Northern Michigan University, and Mrs. Susan A. Brotherton for assistance with the mass spectra. A generous allotment of computer time was provided by the University of Arizona Computer Center.

Registry No. *trans*-Di-*tert*-butyl hyponitrite, 82554-97-0; *tert*-butyl hyponitrite, 82554-98-1; $Na_2N_2O_2$, 82554-99-2; $NaNO_2$, 68378-96-1.

(27) Durig, J. R.; Craven, S. M.; Mulligan, J. H.; Hawley, C. W.; Bragin, J. *J. Chem. Phys.* **1973**, *58*, 1281–91.

Absolute Rate Constants for the Addition of Triethylsilyl Radicals to the Carbonyl Group[1]

C. Chatgilialoglu,[2] K. U. Ingold,* and J. C. Scaiano

Contribution from the Division of Chemistry, National Research Council of Canada, Ottawa, Ontario, Canada K1A 0R6. *Received December 28, 1981*

Abstract: The absolute rate constants for the reactions of $Et_3Si\cdot$ radicals with a large number of carbonyl-containing compounds have been measured in solution by using laser flash photolysis for compounds having rate constants $>10^5$ M^{-1} s^{-1} and kinetic EPR spectroscopy for compounds having rate constants $<10^5$ M^{-1} s^{-1}. The reactivities have a wide range, e.g., the rate constants at ca. 300 K are 2.5×10^9, 3.3×10^8, 1.6×10^6, 2.8×10^5, and 3.5×10^4 M^{-1} s^{-1} for duroquinone, benzil, propionic anhydride, diethyl ketone, and ethyl formate, respectively. Arrhenius parameters were determined for a few representative substrates. Thus for benzil, $E_a = (1.02 \pm 0.09)$ kcal/mol and $\log (A/M^{-1} s^{-1}) = 9.26 \pm 0.07$. Polar effects are very important in determining the reactivity of carbonyl-containing compounds toward $Et_3Si\cdot$ radicals; e.g., reactivities are greatly enhanced by neighboring perfluoralkyl and acyloxy groups.

It has been known for some years that silanes add across the carbonyl group of ketones in the presence of free radical initiators[3,4] and that the products formed indicate that the silyl radical adds to the oxygen atom of the carbonyl group.[4] The occurrence of

0002-7863/82/1504-5119$01.25/0